

# Microwave dielectric ceramic of $\text{LiZnPO}_4$ for LTCC applications

C. C. Xia<sup>1</sup> · D. H. Jiang<sup>1</sup> · G. H. Chen<sup>1</sup> · Y. Luo<sup>1</sup> · B. Li<sup>1</sup> · C. L. Yuan<sup>1</sup> · C. R. Zhou<sup>1</sup>

Received: 22 January 2017 / Accepted: 22 April 2017  
© Springer Science+Business Media New York 2017

**Abstract** The feasibility of  $\text{LiZnPO}_4$  (LZP) ceramic prepared by a solid-state reaction method for low-temperature co-fired ceramic application was investigated. Dense ceramic with 94.37% relative density was obtained when the ceramic was sintered at 850 °C for 4 h. The LZP ceramic sintered at 850 °C for 4 h possessed a relative permittivity ( $\epsilon_r$ ) of 5.3 and high quality factor ( $Q \times f$ ) of 28,496 GHz (at 12.9 GHz) with a temperature coefficient of resonant frequency ( $\tau_f$ ) of  $-80.4$  ppm/°C. The relatively large negative  $\tau_f$  value was reduced by adding  $\text{TiO}_2$  into LZP ceramics. The microstructure, microwave dielectric properties and cofiring compatibility with silver of LZP– $\text{TiO}_2$  composites were discussed. The composite with 0.17 volume fraction of  $\text{TiO}_2$  sintered at 950 °C for 4 h shows  $\epsilon_r = 10.0$ ,  $Q \times f = 10,025$  GHz,  $\tau_f = +1.6$  ppm/°C. The LZP– $\text{TiO}_2$  composite was chemically compatible with the commonly used electrode material silver.

## 1 Introduction

With the rapid development of microwave telecommunication industry, various microwave dielectric materials and devices such as duplexers, resonators, antennas and oscillators, have been widely used and investigated for several decades [1]. Meanwhile, the widespread use of microwave communication accelerated the search for new technologies to produce miniaturized microwave devices. Among the latest technologies, low-temperature co-fired ceramics

(LTCC) technology has proven its potential in developing high-density, low-cost modules for high-performance electronic systems and is required for miniaturization and integration of microwave components for wireless communication [2]. The material selection plays a crucial role in determining the final performance of the modules. As we know, microwave dielectric materials should possess low dielectric constant ( $\epsilon_r$ ), low loss (high quality factor [ $Q \times f$ ],  $Q = 1/\tan \delta$ ,  $f$  = microwave frequency) and near zero temperature coefficient of resonant frequency ( $\tau_f$ ) in order to utilize them as microwave dielectric for microwave communication [3, 4]. Furthermore, the microwave dielectric materials for LTCC applications have to be sintered below the melting point (961 °C) to actualize co-firing with conventional cheap silver (Ag) electrode. To reduce the firing temperature of microwave dielectric materials, there are basically two effective methods: (i) the addition of low melting oxides and glasses into the ceramic, and (ii) the use of ultra fine powders synthesized through wet chemical processing. The decrease of  $Q \times f$ , however, is chief shortcoming for the first method. For the second method, complex process and high cost undoubtedly limit its application. The most competitive method is to use ceramics having inherent low densification temperature. Therefore, there is an ever-growing need for novel additive-free microwave ceramics with good dielectric properties and low firing temperature.

Recently, some lithium-transition metal phosphates  $\text{LiMPO}_4$  ( $M = \text{Fe, Mn, Co, Ni}$ ) with olivine structure were reported to be attractive for LTCC applications because these compounds have relatively low melting point and can be sintered below 900 °C [5]. However, most investigation is focused on the electrochemical and illuminant properties of the  $\text{LiMPO}_4$  [6, 7]. More recently, Hu et al. [8] studied dielectric relaxation and microwave dielectric

✉ G. H. Chen  
cgh1682002@163.com; chengh@guet.edu.cn

<sup>1</sup> School of Materials Science and Engineering, Guilin University of Electronic Technology, Guilin 541004, China

properties of low sintered  $\text{LiMnPO}_4$  ceramics. However, large negative value (90–101 ppm/ $^{\circ}\text{C}$ ) restricts its practical application. And the compatibility of the  $\text{LiMnPO}_4$  ceramic with an Ag electrode had not been studied. Thomas et al. [9] reported  $\text{LiMgPO}_4$  ( $\epsilon_r=6.6$ ,  $Q \times f=79,100$  GHz, and  $\tau_f=-55$  ppm/ $^{\circ}\text{C}$ ) ceramic can be cofired with silver. To date, there are no reports on the microwave dielectric properties of  $\text{LiZnPO}_4$  (LZP) for LTCC applications.

In this work, LZP ceramic was prepared via the solid state reaction method for the first time. The firing, microstructure, microwave dielectric properties were systematically studied. Moreover, to further improve the dielectric properties,  $\text{TiO}_2$  was selected to tune the temperature coefficient of resonant frequency ( $\tau_f$ ) to near zero and increase the permittivity ( $\epsilon_r$ ) as well as not deteriorate and  $Q \times f$  value. Meanwhile, the influences of  $\text{TiO}_2$  additive on the phase purity, microstructure, and microwave dielectric properties of LZP ceramics, and the compatibility of the LZP- $\text{TiO}_2$  composite with an Ag electrode have also been studied. These new LTCC ceramic materials with good microwave dielectric properties can address the growing demand of LTCC technology.

## 2 Experimental procedures

$\text{LiZnPO}_4$  (LZP) ceramic was synthesized by the conventional solid state reaction route. Analytical grade powders of  $\text{Li}_2\text{CO}_3$ ,  $\text{ZnO}$ ,  $\text{NH}_4\text{H}_2\text{PO}_4$  and  $\text{TiO}_2$  were used as the starting materials. The raw oxide materials were weighted according to the stoichiometric ratio and ball milled in ethanol medium for 4 h in nylon jars using yttria stabilized zirconia balls. The mixture was calcined at  $600^{\circ}\text{C}$  in air for 4 h. The calcined LZP powders were remilled together with different volume percentages of  $\text{TiO}_2$  (14–21 vol%) in alcohol medium for 24 h. After drying, and mixing with 5 wt% polyvinyl alcohol (PVA) solution, the granulated powders were pressed uniaxially into pellets of 12 mm in diameter and 6–7 mm in thickness under a pressure of 100 MPa. The pellets were then fired at  $600^{\circ}\text{C}$  for 1 h to expel the binder before sintering at temperatures in the range of  $775$ – $950^{\circ}\text{C}$  for 4 h in air.

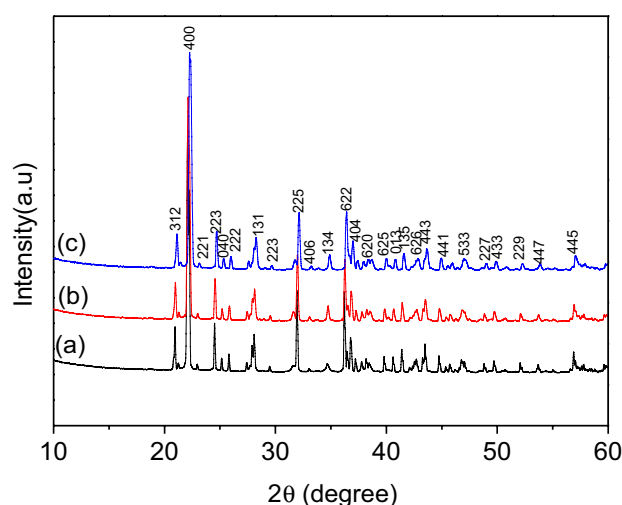
The bulk density was measured by using the Archimedes method. The phase structure was identified by X-ray diffraction (XRD) technique using  $\text{CuK}\alpha$  radiation (Bruker D8 Advance, Germany). The surface microstructure of the specimens was evaluated by field scanning electron microscopy (SEM) (Quanta 600 FEG, FEI) coupled with energy-dispersive X-ray spectroscopy (EDS). Dielectric behaviors at microwave frequency were measured with the  $\text{TE}_{018}$  shielded cavity method with a network analyzer (N5230C, Agilent, Palo Alto, CA) and a temperature chamber (Delta 9023, Delta Design, Poway, CA) in the temperature range

of  $25$ – $75^{\circ}\text{C}$ . The temperature coefficient of resonant frequency ( $\tau_f$ ) was measured by noting the variation of resonant frequency of the  $\text{TE}_{011}$  resonant mode over the temperature range. To check the chemical compatibility between the ceramic and the silver powder, 20 wt% silver was mixed with the LZP +  $\text{TiO}_2$  powder, and then the pressed pellets were fired at  $900^{\circ}\text{C}$  for 4 h to achieve equilibrium.

## 3 Results and discussion

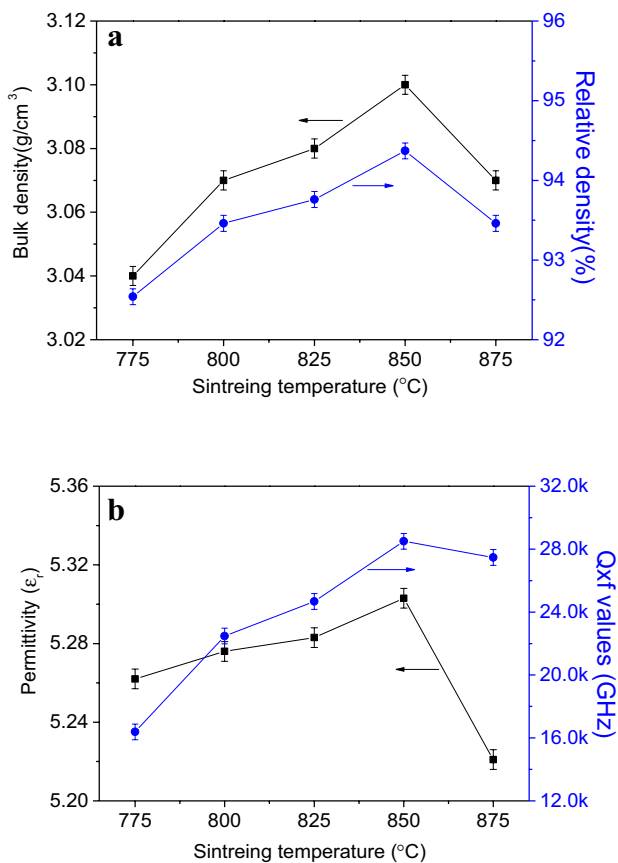
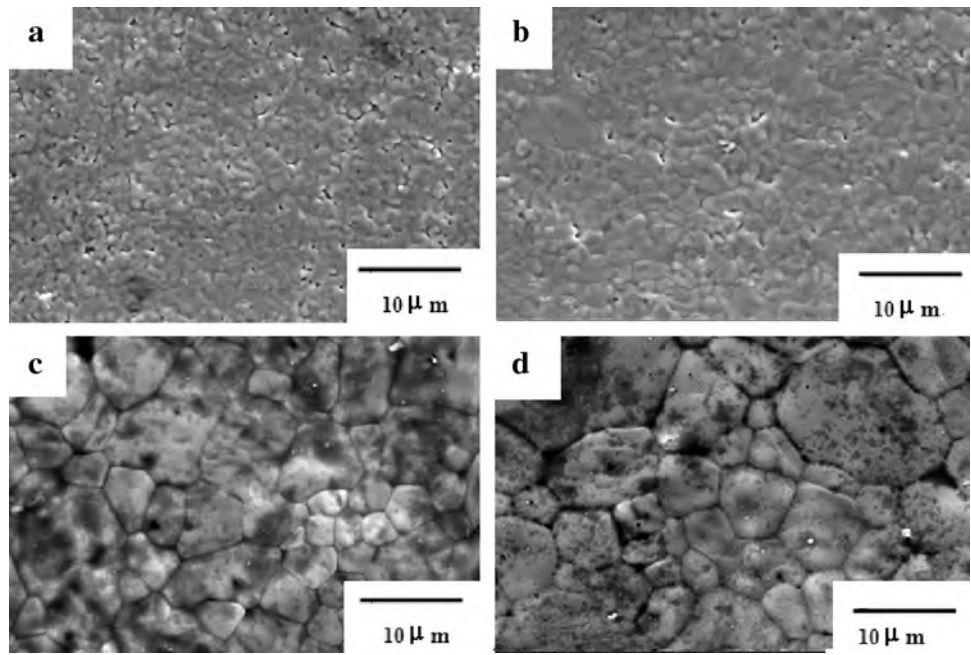
Figure 1 shows the powder XRD patterns of LZP ceramics sintered at various temperatures for 4 h. All the diffraction peaks are indexed JCPDS file number 79-0804 for  $\text{LiZnPO}_4$ , and no additional peaks are observed. The SEM micrographs of the surface for pure LZP ceramic sintered at different temperatures 4 h are depicted in Fig. 2. At  $775^{\circ}\text{C}$ , the sample presents not too dense microstructure with average grain size of  $1\text{ }\mu\text{m}$  shown in Fig. 2a. Raising temperature leads to the porosity decreasing and grain size increasing seen in Fig. 2b–d. At  $850^{\circ}\text{C}$ , the dense uniform microstructure with average grain size of  $5\text{ }\mu\text{m}$  is observed and the grain boundary is clear, as shown in Fig. 2c. With further increasing temperature to  $875^{\circ}\text{C}$ , obviously asymmetrical microstructure is formed shown in Fig. 2d, which is probably owing to excessive sintering temperature resulting in slightly evaporation of Li during firing process.

Figure 3a shows the bulk and relative densities of LZP ceramic as a function of sintering temperature. The bulk and relative densities display a similar variation trend with the increment of temperature. The theoretical density of the  $\text{LiZnPO}_4$  ceramic is  $3.285\text{ g cm}^{-3}$  [10]. The maximal relative density of 94.37% at  $850^{\circ}\text{C}$



**Fig. 1** XRD patterns of LZP ceramics sintered at various temperatures for 4 h: a  $775^{\circ}\text{C}$ , b  $850^{\circ}\text{C}$ , c  $875^{\circ}\text{C}$

**Fig. 2** SEM images of the  $\text{LiZnPO}_4$  ceramic sintered at various temperatures for 4 h: **a** 775 °C, **b** 800 °C, **c** 850 °C, **d** 875 °C



**Fig. 3** **a** Variation of bulk density and relative density of LZF ceramics, **b** permittivity ( $\epsilon_r$ ) and  $Q \times f$  values of LZF ceramics as a function of sintering temperature

is reached. The decrease of relative density at 875 °C may be due to over-burning and heterogeneous exaggerated grain growth. The changes in permittivity and  $Q \times f$  value of the ceramics with firing temperature are illustrated in Fig. 3b. It is observed that the permittivity firstly increases, reaches a maximum value of 5.3 at 850 °C, and then decreases with increasing temperature. Generally, the permittivity at microwave frequency depends on the relative density and secondary phases, etc [11]. The effect of secondary phase on the permittivity can be neglected since there is no any secondary phase in XRD patterns. The variation in permittivity with sintering temperature is in well agreement with that in relative density. It is clear that the saturation of  $Q \times f$  value occurs at 850 °C shown in Fig. 3b. The  $Q \times f$  value decreases with further increase of sintering temperature, which may be attributed to the low densification. The as-prepared LZF ceramic sintered at 850 °C possesses a ultimate  $Q \times f$  value of 28,496 GHz (at 12.9 GHz) and a relatively large negative value of  $\tau_f$  (−80.4 ppm/°C). Apparently, its high negative  $\tau_f$  is not suitable for practical applications. The big negative value of  $\tau_f$  can be lowered by introducing  $\text{TiO}_2$  with a high-positive  $\tau_f$  (~450 ppm/°C) in the LZF ceramics.

Figure 4 shows the XRD patterns of LZF– $\text{TiO}_2$  composites with various volume percentage of  $\text{TiO}_2$  sintered at 950 °C for 4 h. It is found that the mixture of  $\text{LiZnPO}_4$  (PDF#79-0804) and  $\text{TiO}_2$  (PDF#21-1276) coexists for all the compositions, and no other phases are observed. This means that no chemical reaction between LZF and  $\text{TiO}_2$  occurs. The big difference in crystal structure and good stability of both phases restrain the chemical reaction between LZF and  $\text{TiO}_2$  [12].

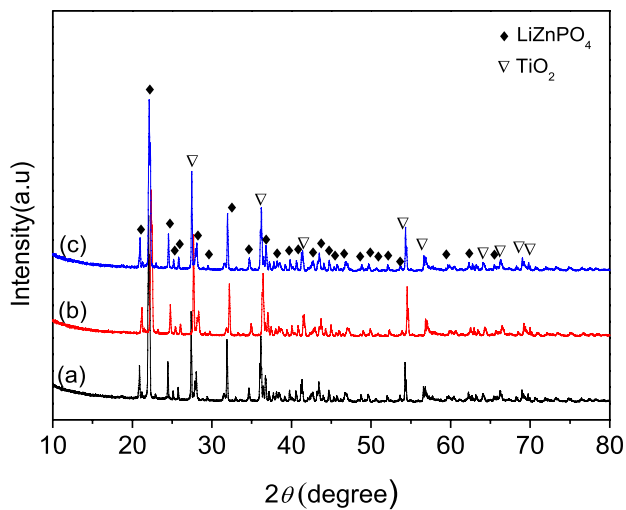


**Fig. 4** XRD patterns of LZP–TiO<sub>2</sub> composites with different volume fraction of TiO<sub>2</sub> sintered at 950 °C 4 h: *a* 0.15, *b* 0.17, *c* 0.19

Figure 5 shows the SEM micrographs of LZP–TiO<sub>2</sub> composites with different volume percentage of TiO<sub>2</sub> sintered at 950 °C for 4 h. All the samples containing TiO<sub>2</sub> exhibit a pronounced difference in microstructure compared with the specimen without TiO<sub>2</sub> shown in Fig. 2c, namely, both of large grains and fine grains coexist, as shown in Fig. 5. As a whole, all the samples present a dense microstructure. However, adding 0.19 volume fraction of TiO<sub>2</sub> has somewhat adverse effect on the densification. It is well known that the melting point of TiO<sub>2</sub> is very high (>1800 °C) [13]. Hence, the diffusion rate of ions is very low at low sintering temperature. It is guessed that the grain refining may be

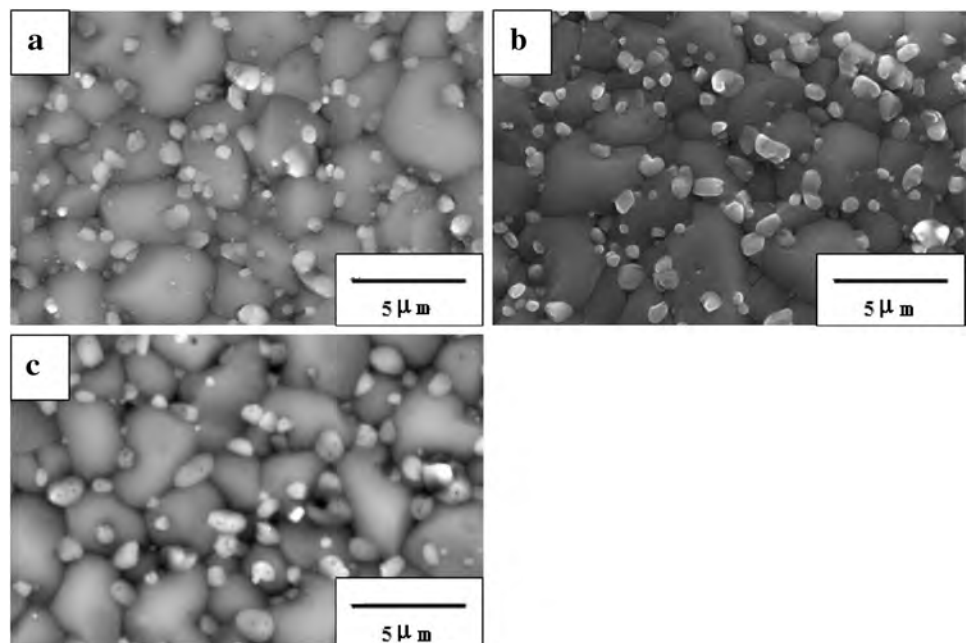
owing to the function of TiO<sub>2</sub>. In other words, the addition of TiO<sub>2</sub> increase the sintering temperature and change the grain morphology and grain size.

The microwave dielectric properties of LZP–TiO<sub>2</sub> composites sintered at 950 °C for 4 h are listed in Table 1. With the increment of TiO<sub>2</sub>, the permittivity of the composites increases, which is due to that TiO<sub>2</sub> has a large value of  $\epsilon_r$  (~100) [13]. A reduction in  $Q \times f$  with the increase in TiO<sub>2</sub> volume fraction may be mainly due to the following reasons: (i) the decrease in the densification. (ii) possible electrical inhomogeneity produced by the mixing of two materials with largely different  $\epsilon_r$  values. (iii) nonuniform mixing of phases causing detrimental effects on  $Q \times f$ . The  $\tau_f$  is well known to be governed by the composition. Because the  $\tau_f$  values of the LZP and TiO<sub>2</sub> are about negative 80 ppm/°C and positive 411 ppm/°C, respectively, the increment of TiO<sub>2</sub> content makes the  $\tau_f$  value become more positive. It implies that zero  $\tau_f$  can be easily achieved by adjusting the amount of

**Table 1** Microwave properties of LiZnPO<sub>4</sub>–TiO<sub>2</sub> composites with different volume fraction of TiO<sub>2</sub> fired at 950 °C for 4 h

Volume fraction of TiO <sub>2</sub>	$\epsilon_r$	$Q \times f$ (GHz)	$\tau_f$ (ppm/°C)
0	5.5	28,496	−80.2
0.14	8.3	13,844	−24.0
0.15	8.8	11,769	−21.5
0.17	10.0	10,025	1.6
0.19	10.7	10,552	7.8
0.21	10.9	10,738	24.3

**Fig. 5** SEM images of LZP–TiO<sub>2</sub> composites with different volume fraction of TiO<sub>2</sub> sintered at 950 °C for 4h: *a* 0.15, *b* 0.17, *c* 0.19





TiO<sub>2</sub> content. Typically, the LZP with 0.17 volume fraction of TiO<sub>2</sub> has good microwave dielectric properties of  $\epsilon_r = 10.0$ ,  $Q \times f = 10,025$  GHz,  $\tau_f = 1.6$  ppm/°C, as shown in Table 1. Further investigations are required to improve the  $Q \times f$  value for application in wireless communication systems.

The theoretical permittivity ( $\epsilon_r$ ) of LiZnPO<sub>4</sub>-TiO<sub>2</sub> composites with different volume fraction of TiO<sub>2</sub> sintered at 950 °C for 4 h can be calculated using different existing models and expression. The mathematical equations of each model are described as follows:

Series mixing model [14]:

$$\frac{1}{\epsilon_r} = \frac{(1-x)}{\epsilon_{r_1}} + \frac{x}{\epsilon_{r_2}} \quad (1)$$

Paralell mixing model [15]:

$$\epsilon_r = (1-x)\epsilon_{r_1} + x\epsilon_{r_2} \quad (2)$$

Lichtenecker model [16]:

$$\ln \epsilon_r = (1-x) \ln \epsilon_{r_1} + x \ln \epsilon_{r_2} \quad (3)$$

where  $x$  is the volume fraction of TiO<sub>2</sub>,  $\epsilon_{r_1}$  and  $\epsilon_{r_2}$  are the dielectric constant of LZP and TiO<sub>2</sub>, respectively. The theoretical and measured dielectric constants of LZP-TiO<sub>2</sub> composites sintered at 950 °C for 4 h are described in Fig. 6. By comparing the experimentally observed values of  $\epsilon_r$  with the predicted values, only Lichtenecker model is comparatively closer to the measured results. However, the theoretical value and experimental value exists a certain deviation. The deviation of  $\epsilon_r$  from the predicted mixing relations may be due to not only the dissimilar microstructural grain morphologies of both phases but also the presence of porosity [17, 18].

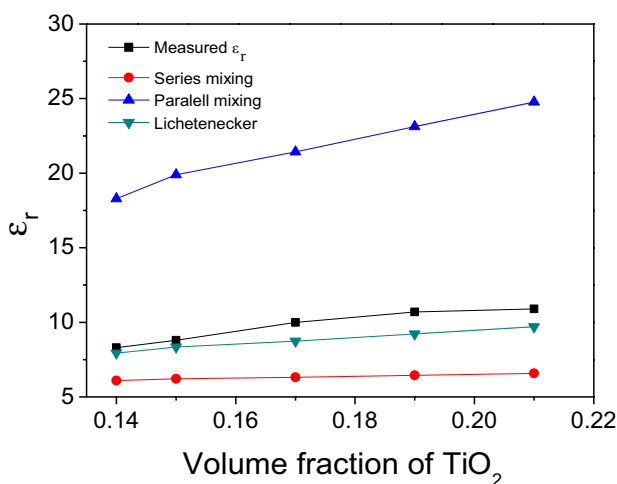


**Fig. 6** Theoretical and measured dielectric constant of LZP-TiO<sub>2</sub> composites with different volume fraction of TiO<sub>2</sub> sintered at 950 °C for 4 h

Figure 7 shows the variation of experimental and calculated values of  $\tau_f$  with the volume fractions of TiO<sub>2</sub>. According to the Lichtenecker empirical rule [16], the value of  $\tau_f$  for the composites can be predicted using the mixture rule:

$$\tau_f = v_1 \tau_{f1} + v_2 \tau_{f2} \quad (4)$$

where  $v_1$  and  $v_2$  are the volume fractions of LZP and TiO<sub>2</sub>,  $\tau_{f1}$  and  $\tau_{f2}$  are the  $\tau_f$  values of LZP and TiO<sub>2</sub>, respectively. It is observed that both the theoretical  $\tau_f$  values and the measured  $\tau_f$  values increase with the increasing  $x$  value, and the change of the theoretical and measured  $\tau_f$  values exhibits similar behavior. Clearly, a near zero  $\tau_f$  value can

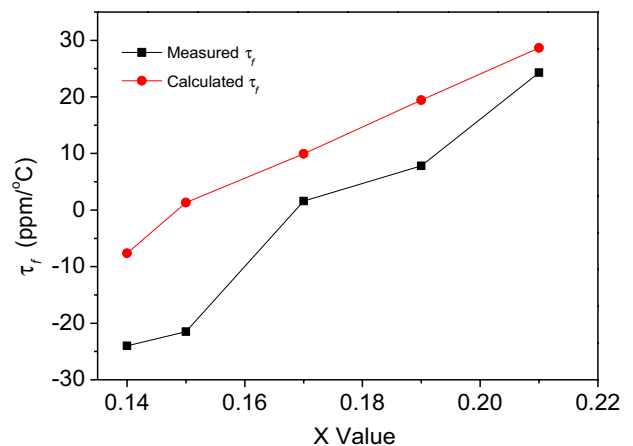


**Fig. 7** Temperature coefficient of resonant frequency ( $\tau_f$ ) of LiZnPO<sub>4</sub>-TiO<sub>2</sub> composite as a function of volume fraction of TiO<sub>2</sub>

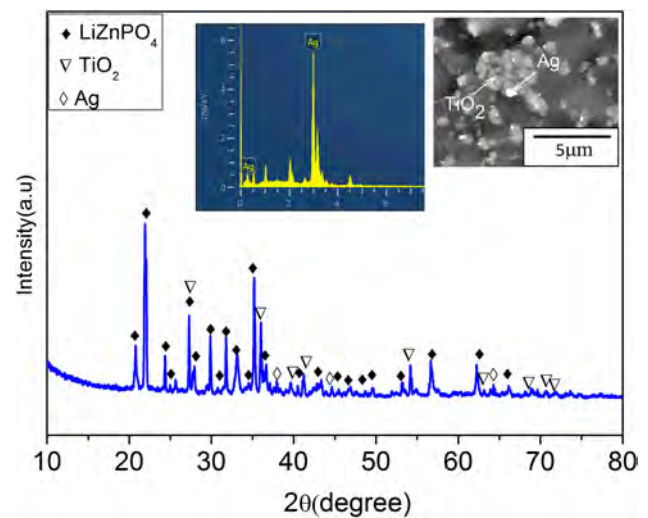


**Fig. 8** XRD patterns of LZP -0.17 TiO<sub>2</sub>+20 wt% Ag sintered at 900 °C for 4 h. The insets show the EDS and SEM image of this specimen

be obtained as  $x$  is in the vicinity of 0.17, as shown in Fig. 7 and Table 1. However, the theoretical  $\tau_f$  and experimental  $\tau_f$  exists a certain deviation, which may be due to the differences in crystal microstructure of LZP and  $\text{TiO}_2$  phases.

Figure 8 depicts XRD patterns, EDS result and SEM profile of LZP  $-0.17 \text{ TiO}_2 + 20 \text{ wt\% Ag}$  sintered at  $900^\circ\text{C}$  for 4 h. From the XRD pattern, co-firing with Ag powders does not produce a new phase other than metallic silver, LZP (matrix) and  $\text{TiO}_2$  in the sample. This observation is also confirmed by the SEM and EDS analysis (Fig. 8). The SEM analysis indicates no interaction forming new phases after firing, and it is obvious that the reaction of ceramics and Ag powders does almost not occur from the EDS result. Hence, this would benefit commercial applications in LTCC field.

## 4 Conclusions

LZP ceramic was fabricated through a solid-state reaction method. LZP ceramic fired at  $850^\circ\text{C}$  for 4 h shows good dielectric properties of  $\epsilon_r=5.3$ ,  $Q \times f=28,496 \text{ GHz}$ , and  $\tau_f=-80.4 \text{ ppm}^\circ\text{C}$ . By adding  $\text{TiO}_2$  in the LZP ceramic, the large negative value of  $\tau_f$  can be facilely tune to near zero. Typically, the LZP+ $0.17 \text{ TiO}_2$  (volume fraction) sintered at  $950^\circ\text{C}$  for 4 h has  $\epsilon_r=10.0$ ,  $Q \times f=10,025 \text{ GHz}$ ,  $\tau_f=1.6 \text{ ppm}^\circ\text{C}$ . The merit for the  $\text{TiO}_2$ -added LZP ceramic is its good compatibility with the Ag electrode. These finding suggest the as-prepared ceramics could be a promising candidate for LTCC applications.

**Acknowledgements** This work was financially supported by the National Natural Science Foundation of China (Grant No. 51462005), the Research funds of The Guangxi Key Laboratory of Information Materials (Nos. 131018-Z and 131004-Z), Program for Postgraduate Joint Training Base (No. 20160513-14-Z) and Project supported by National Undergraduate Innovation Program of the Ministry of Education of China (1401010113).

## References

1. B. Tang, X. Guo, S.Q. Yu, Z.X. Fang, S.R. Zhang, The shrinking process and microwave dielectric properties of  $\text{BaCu}(\text{B}_2\text{O}_5)$ -added  $0.85\text{BaTi}_4\text{O}_9-0.15\text{BaZn}_2\text{Ti}_4\text{O}_{11}$  ceramics. *Mater. Res. Bull.* **66**, 163–168 (2015)
2. X. Tang, H. Yang, Q.L. Zhang, J.H. Zhou, Low-temperature sintering and microwave dielectric properties of  $\text{ZnZrNb}_2\text{O}_8$  ceramics with  $\text{BaCu}(\text{B}_2\text{O}_5)$  addition. *Ceram. Int.* **40**, 12875–12881 (2014)
3. G. Dou, D.X. Zhou, M. Guo, S.P. Gong, Low-temperature sintered  $\text{Zn}_2\text{SiO}_4\text{-CaTiO}_3$  ceramics with near-zero temperature coefficient of resonant frequency. *J. Alloys Compd.* **513**, 466–473 (2012)
4. G.H. Chen, M.Z. Hou, Y. Yang, Microwave dielectric properties of low-fired  $\text{Li}_2\text{TiO}_3$  ceramics doped with  $\text{Li}_2\text{O-MgO-B}_2\text{O}_3$  frit. *Mater. Lett.* **89**, 16–18 (2012)
5. S.Y. Chung, J.T. Bloking, Y.M. Chiang, Electronically conductive phosphor-olivines as lithium storage electrodes. *Nat. Mater.* **1**, 123–128 (2002)
6. Q. Yu, H.D. Zeng, Q. Jiang, Z. Liu, L.Y. Sun, J. Ren, G.R. Chen, Preparation and luminescent properties of  $\text{Mn}^{2+}$  doped glass and glass-ceramics containing  $\text{LiZnPO}_4$  nanocrystals. *J. Non-Cryst. Solids* **35**(4), 165–168 (2014)
7. C.M. OuYang, M.A. Shuai, Y. Rao, X. Zhou, X. Zhou,  $\text{LiZnPO}_4\text{:Tb}^{3+}$ ,  $\text{Ce}^{3+}$ , green phosphors with high efficiency. *J. Rare Earths* **30**(7), 637–640 (2012)
8. X. Hu, Z.F. Cheng, Y. Li, Z.Y. Ling, Dielectric relaxation and microwave dielectric properties of low temperature sintering  $\text{LiMnPO}_4$  ceramics. *J. Alloys Compd.* **651**, 290–293 (2015)
9. D. Thomas, M.T. Sebastian, Temperature-compensated  $\text{LiMgPO}_4$ : A new glass-free low-temperature cofired ceramic. *J. Am. Ceram. Soc.* **93**, 3828–3831 (2010)
10. J.A. Gard, G. Torres-Trevino, A.R. West, Crystal data for  $\text{LiZnPO}_4$ . *J. Mater. Sci. Lett.* **4**, 1138–1139 (1985)
11. D. Zhou, L.X. Pang, X. Yao, H. Wang, Influence of sintering process on the microwave dielectric properties of  $\text{Bi}(\text{V}_{0.008}\text{Nb}_{0.992})\text{O}_4$  ceramics. *Mater. Chem. Phys.* **115**, 126–131 (2009)
12. G. Chen, M. Hou, Y. Bao, C.L. Yuan, C.R. Zhou, H.R. Xu, Silver co-firable  $\text{Li}_2\text{ZnTi}_3\text{O}_8$ , microwave dielectric ceramics with LZB glass additive and  $\text{TiO}_2$  dopant. *Int. J. Appl. Ceram. Technol.* **10**(3), 492–501 (2013)
13. C.H. Hsu, H.A. Ho, Microwave dielectric in the  $\text{Sm}(\text{Co}_{1/2}\text{Ti}_{1/2})\text{O}_3\text{-CaTiO}_3$  ceramic system with near-zero temperature coefficient with resonant frequency. *Mater. Lett.* **64**, 396–398 (2010)
14. D. Borrow, T. Petroff, R. Tandon, M. Sayer, Slab plasmon polaritons and waveguide modes in four-layer resonant semiconductor waveguides. *J. Appl. Phys.* **81**, 8761 (1997)
15. P. Sarah, S.V. Suryanarayana, Dielectric properties of piezoelectric 3–0 composites of lithium ferrite/barium titanate. *Bull. Mater. Sci.* **26**(7), 745–747 (2003)
16. K. Lichteneker, Dielectric constant of natural and synthetic mixtures. *Phys. Z* **27**(1926)115
17. H.H.B. Rocha, F.N.A. Freire, M.R.P. Santos, Radio-frequency (RF) studies of the magneto-dielectric composites:  $\text{Cr}_{0.75}\text{Fe}_{1.25}\text{O}_3(\text{CRFO})\text{-Fe}_{0.5}\text{Cu}_{0.75}\text{Ti}_{0.75}\text{O}_3(\text{FCTO})$ . *Phys. B* **403**(17), 2902–2909 (2008)
18. D.W. Kim, H.J. Youn, K.S. Hong, C.K. Kim, Microwave dielectric properties of  $(1-x)\text{Ba}_5\text{Nb}_4\text{O}_{15}\text{-xBaNb}_2\text{O}_6$  mixtures. *Jpn. J. Appl. Phys.* **41**, 3812–3816 (2002)